

Isospin Mixing in ^{18}F

H. T. RICHARDS

University of Wisconsin, Madison

1. Introduction

In 1932, shortly after the **discovery** of the neutron, Heisenberg¹ introduced an isotopic **spin** notation for bookkeeping **purposes** on neutron and protons. However, the **formalism** lacked any other physical content.

In 1936, **analyses** of p - p scattering **showed** a striking agreement of the 1S state pp force with the 1S state np force and Breit and Feenberg² emphasized the possibility that **all** interactions **between** nucleons were the same, except for the Coulomb effects and the **Pauli** exclusion **principle**.

Soon afterward (1937), **Wigner**³ adapted this suggestion of complete charge **independence** to his supermultiplet theory and introduced a total isospin quantum number T to label different states of isobaric multiplets.

Although the isospin quantum number had a few immediately useful applications, there **was** so little reliable experimental information about nuclear levels in isobars that the great beauty **and usefulness** of Wigner's isospin lay largely dormant until well after World War II. In 1952, Bob Adair⁴ at the University of Wisconsin **revived** interest in the isospin concept by his now **classic** paper where he explicitly pointed out many experimental consequences of isospin conservation. In fact Bob Adair's paper **was** in part prompted by some peculiar experimental results which some of my students **observed** (or rather **failed** to observe). They were using a **spherical** electrostatic analyzer to measure reaction energies and energy levels to a **high precision**. **Earlier** we had measured the $^{16}\text{O}(d, \alpha)^{14}\text{N}$ ground state reaction, but we puzzled over our inability to **detect** the same reaction going to the **first** excited state of ^{13}N . Bob Adair **recognized** immediately that the forbiddenness was in some way connected with this excited state being the analog of ^{14}C and ^{14}O ground states, i.e., a member of the lowest $T = 1$ multiplet for $A = 14$.

Figure 1, which shows the **current level** information for **these isobars**⁵, will make the picture more clear.

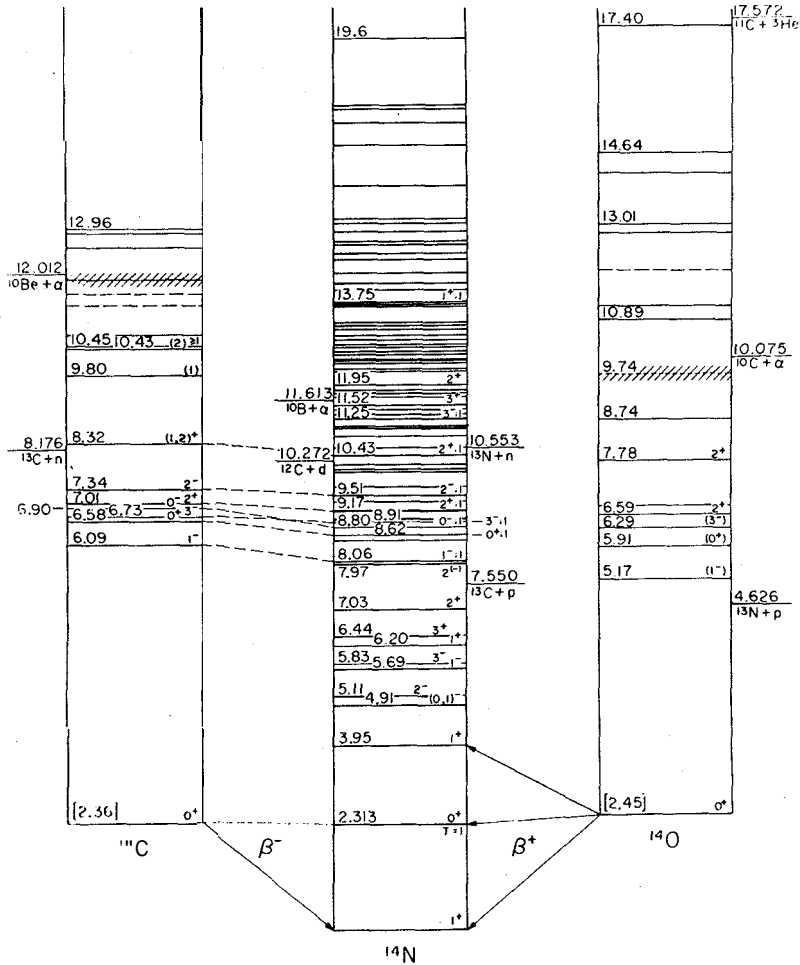


Fig. 1 - Energy levels for the mass 14 isobars.

The middle nucleus ^{14}N is **self-conjugate** in that it contains equal numbers of neutrons and protons. ^{14}C and ^{14}O are mirror nuclei **since** we can go from one to the other by **converting all** protons to neutrons and **all** neutrons to protons. Clearly, if nuclear forces are charge independent, then ^{14}C

and ^{14}O should have the same level structure. The self-conjugate ^{14}N however has more n-p pairs and so the exclusion principle permits numerous states in ^{14}N which are forbidden to the ^{14}C - ^{14}O mirror pair. These exclusively ^{14}N levels we label $T = 0$. Those levels permitted for all three isobars we label $T = 1$ and of course the charge multiplicity of these states is given by $(2T + 1)$ in the same manner that the ordinary spin multiplicity is $(2I + 1)$.

Now, if nuclear forces are charge independent, then this isospin quantum number T must be conserved in a nuclear reaction⁴.

For our case, $^{16}\text{O}(d, \alpha)^{14}\text{N}$, all the nuclei are self conjugate and hence $T = 0$ in their ground states. However, when we try to prepare ^{14}N in its first excited state ($T = 1$) we face the impossible task of combining $T = 0$ systems to give the necessary $T = 1$ state and hence the reaction is isospin forbidden.

Although then we would set only a limit that the isospin-forbidden cross section was less than $1400 \mu\text{barns/sr}$, I urged one of my former students, C. P. Browne, who went as a post-doctorate to M. I. T. to use the magnetic analyzer and the higher deuteron bombarding energy available there to search more carefully for the forbidden reaction. With long exposures

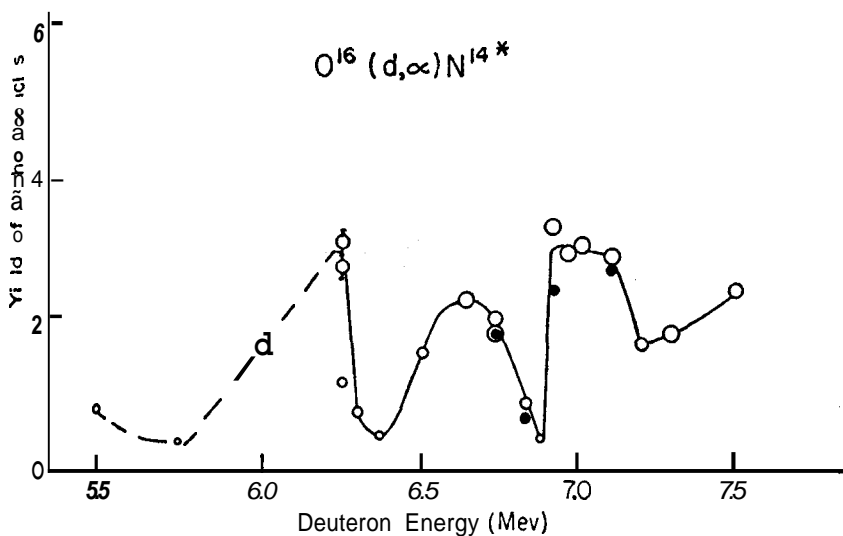


Fig. 2 - Excitation function obtained by C. P. Browne for the reaction $^{16}\text{O}(d, \alpha)^{14}\text{N}^*$ (2.313 MeV).

and much scanning of photographic plates, he did indeed see the reaction. What is more, he obtained a crude excitation curve at one angle. Fig. 2 shows his 1966 results⁶. Note the resonant character of the reaction. These resonances tell us immediately that the states of the compound nucleus are important for understanding the cross section. The compound nucleus in this case is ^{18}F which is of course also a self-conjugate nucleus. Let us therefore turn our attention to ^{18}F .

Figure 3 shows Fay Ajzenberg's most recent but yet unpublished⁷ level diagram of ^{18}F . First, I call your attention to the fact that when we form ^{18}F via the $^{16}\text{O} + \text{d}$ channel, we are in a region of excitation above 7.5 MeV. Here the level density is obviously becoming high. Secondly, I call your attention to Ajzenberg's note about 158 states with $11 < E_x < 20.8 \text{ MeV}$. Most of these (and many others between 9 and 11 MeV) are the isospin mixed states of ^{18}F which we at Wisconsin have recently located and for which we extracted the parameters J^π , the total width Γ and the product of the partial widths, $\Gamma_i \Gamma_o$.

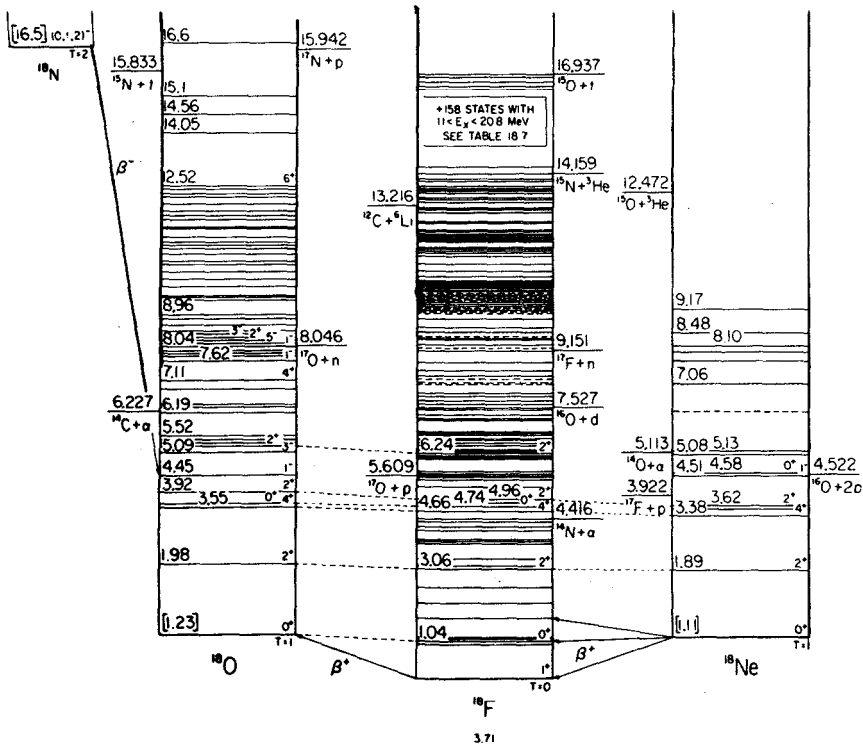


Fig. 3 - Energy levels for the mass 18 isobars.

I devote the next part of this report to **tell** how we obtain this information, and then **finally** we will look at any **systematics** in the results and what we **learn** about nuclear structure and reactions.

Before so doing, let me mention briefly several technological developments which **made** possible this information explosion about ^{18}F states. First **was** the development of the tandem accelerator, which in tum depended upon **Prof. Herb's** development of a practical source of **negative** hydrogen ions^S; second was the development of the **silicon** surface barrier detector which gave resolutions **sufficient** to **negate** the need for the expensive (but small solid angle) magnetic (or electrostatic) particle analyzers and the tedious scanning of photographic plates. The third development was the electronic data processing equipment which culminated in high speed computers for both on-line data handling from detectors at many **angles** and for off-line analysis of the final cross sections. A fourth development important to this particular program **was** the development at **Wisconsin** in 1966 of an abundant source of H e ions which let us prepare the same ^{18}F states via a different entrance channel, namely $^{14}\text{N} + ^4\text{He}$.

Beside the technological developments, the theoretical analysis of the data **was** in a large part dependent on the procedures worked out by one of my gifted **graduate** students, Peter Jolivette, now at the University of Notre **Dame**. In fact most of the work I will report here **comprised** the Ph. D. theses of two students, Philip **Tollefsrud**¹⁰ and Peter **Jolivette**¹¹.

2. Experimental Arrangements

Figure 4 shows top and **side views** of the scattering **chamber**¹⁰ used for **all** our measurements. The chamber contains oxygen gas when we prepare ^{18}F via the $^{16}\text{O} + d$ channel and contains nitrogen gas when the $^{14}\text{N} + \alpha$ channel **is** involved. The pressure **is** ~ 10 -20 Torr. **Instead** of a **foil** to **separate** the gas from the high vacuum **beam** tube, we use a **series** of **small** apertures between which we have fast pumps. The advantages of such a windowless **gas** target, as demonstrated by **Prof. Herb** many years ago, are hard to overstate. The **main ones** are 1) freedom from contamination buildup because of the continuous **flushing**, 2) the thin uniform targets whose thickness **can** be optimally and **easily** adjusted, and 3) the accurate knowledge of the target nuclei per cm^2 so that precise absolute cross sections result. The beam enters from the left and after passing through the chamber stops in a Faraday cup which **is isolated** from **the** gas of the chamber by a thin foil.

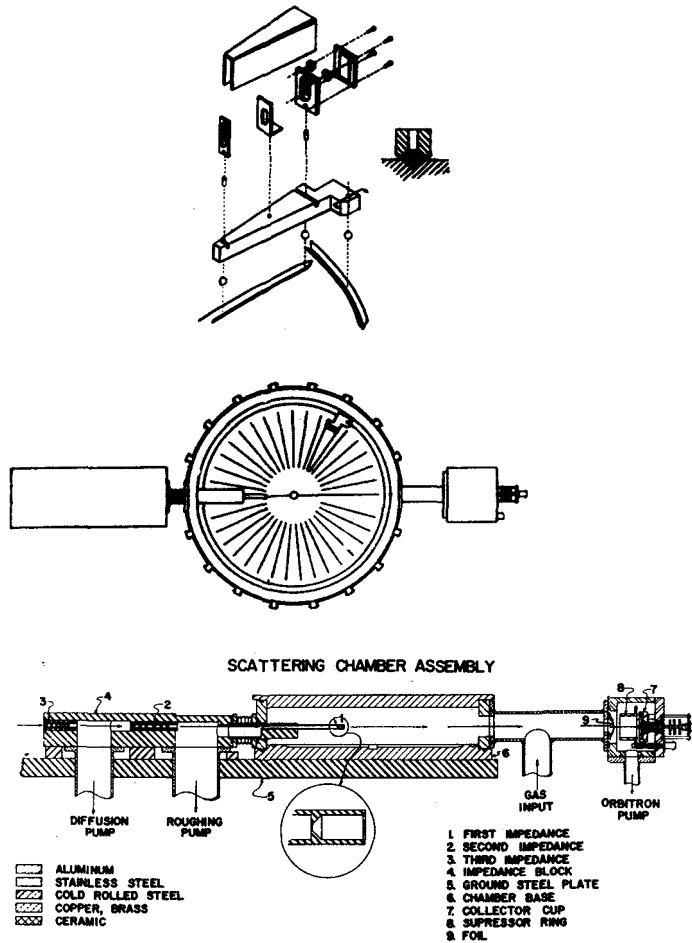


Fig. 4 - Top and side views of the scattering chamber used for the present measurements.

The **surface** barrier type detectors **view** a target volume which is defined by the slit system shown **in** the top of the figure. A kinematic design **reproducibly** locates the slit systems and detectors at angles determined by circumferential and radial V-grooves **milled** in the chamber bottom. We have at times **employed** simultaneously detectors at up to 14 angles.

By choosing detectors with **thin** enough depletion layers we avoid pulses from weakly **ionizing** protons or deuterons which otherwise would obscure

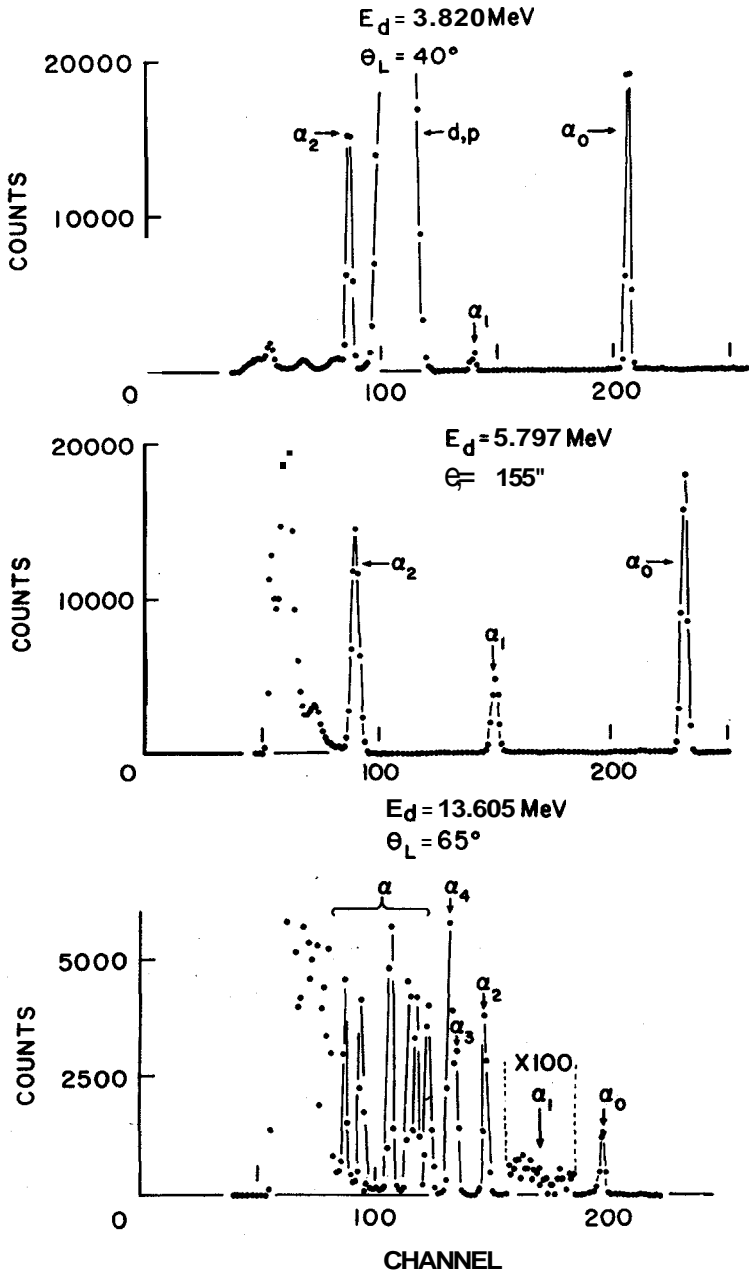


Fig. 5 - Spectra from the $^{16}\text{O} + d$ reactions.

the region where our isospin forbidden alphas must appear. Figure 5 shows several sample spectra** for the $^{16}\text{O} + d$ data. The top spectrum is typical as regards the ratio of the forbidden group, a,, to background and to the allowed groups. The middle spectrum corresponds to our largest measured forbidden cross section ($\sim 3000 \mu\text{b}/\text{sr}$), and the bottom spectrum to a near zero cross section. The background for this particular case would obscure a cross section less than $\sim 0.5 \mu\text{b}/\text{sr}$.

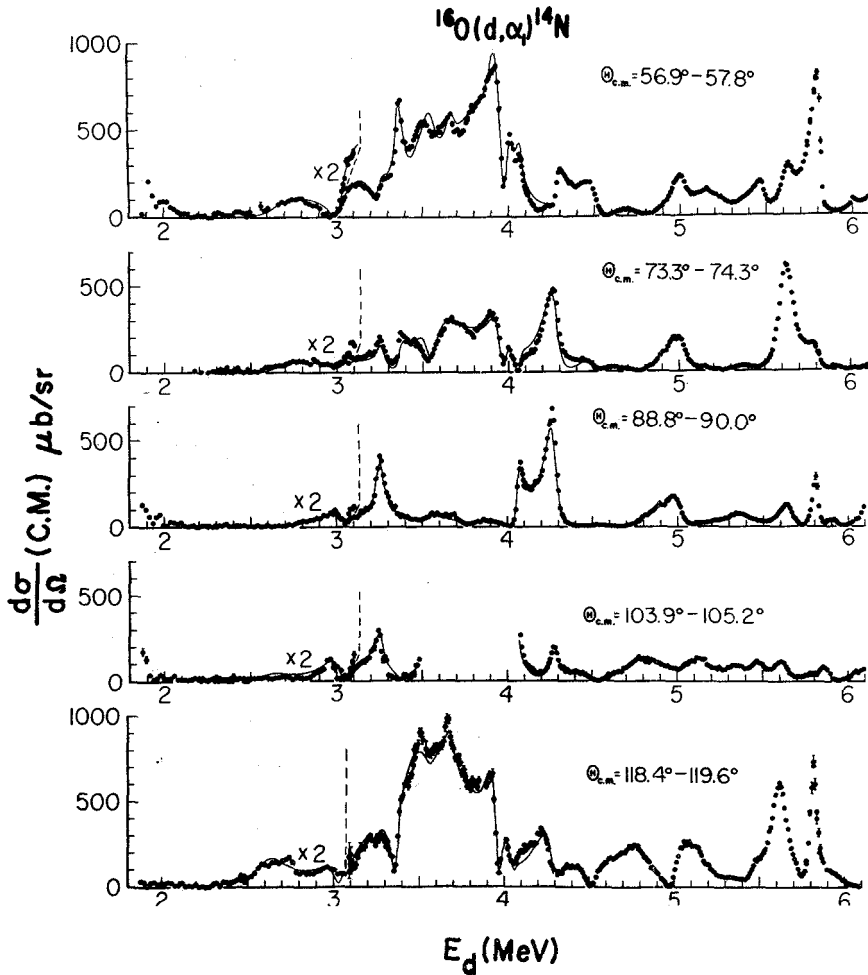


Fig. 6 - Lowest energy excitation functions for the middle angles,

3. Results

We have measured the differential cross sections for the forbidden group from $^{16}\text{O}(d, \alpha)^{14}\text{N}$ from deuteron energies as low as 2 MeV to 14 MeV which is the maximum deuteron energy of our tandem accelerator. The corresponding range of excitation in the compound nucleus ^{18}F is from 9.3 to 20 MeV.

Figure 6 shows a sampling of the lowest energy excitation curves at the middle angles''. Cross sections are reasonably large, backgrounds were low and hence statistics are generally less than the point size. In fact, for all the data subsequently shown, error bars will appear only if they are larger than the point size. Note the relative simplicity of the $\theta_{cm} \simeq 90^\circ$ data compared to the other angles. As we will see later, this simplicity arises because at this angle only $J^\pi = 1^-, 3^-, 5^-$, etc resonances can contribute. In fact, our analysis shows only one 5^- state below 6 MeV and this one occurs at 5.8 MeV. The rest of the peaks arise from 1^- and 3^- levels. The solid line is the theoretical cross section which our extracted level parameters generate. More about this later.

Figure 7 samples the forward angle data'' at middle deuteron energies. Notice the one high point at 6.24 MeV at several angles. This turns out to be an unresolved sharp 4^+ resonance to which I'll refer later. In general, sharp resonance behavior still persists but as the deuteron energy increases the cross sections decrease. The increase in width of the resonances results partially from the superposition of contributions from overlapping levels. For example, analysis shows the intense broad structure at ~ 10.3 MeV to result from a strong pair of 5^- states plus contributions from weaker 3^- , 4^+ , and 6^+ states.

Figure 8 samples our highest energy data'' but at back angles. The trend to smaller cross sections and wider more complex resonances continues but even here we can analyze the data in terms of a relatively few compound nuclear levels.

Figure 9 shows a sample of our data at forward angles for the isospin forbidden $^{14}\text{N}(\alpha, \alpha_1)^{14}\text{N}$ ($T = 1$)^{10,15}. Here we have the same isospin forbidden final system but we enter the ^{18}F compound states by the $^{14}\text{N} + \alpha$ channel. The indicated alpha energies correspond to the ^{18}F excitation energies shown on the top scales of the figures. The intense resonance at $E_\alpha = 12.7$ MeV ($E_\alpha \simeq 10,7$) is the same 5^- state in ^{18}F which we noted earlier on Fig. 6 of the $^{16}\text{O} + d$ data.

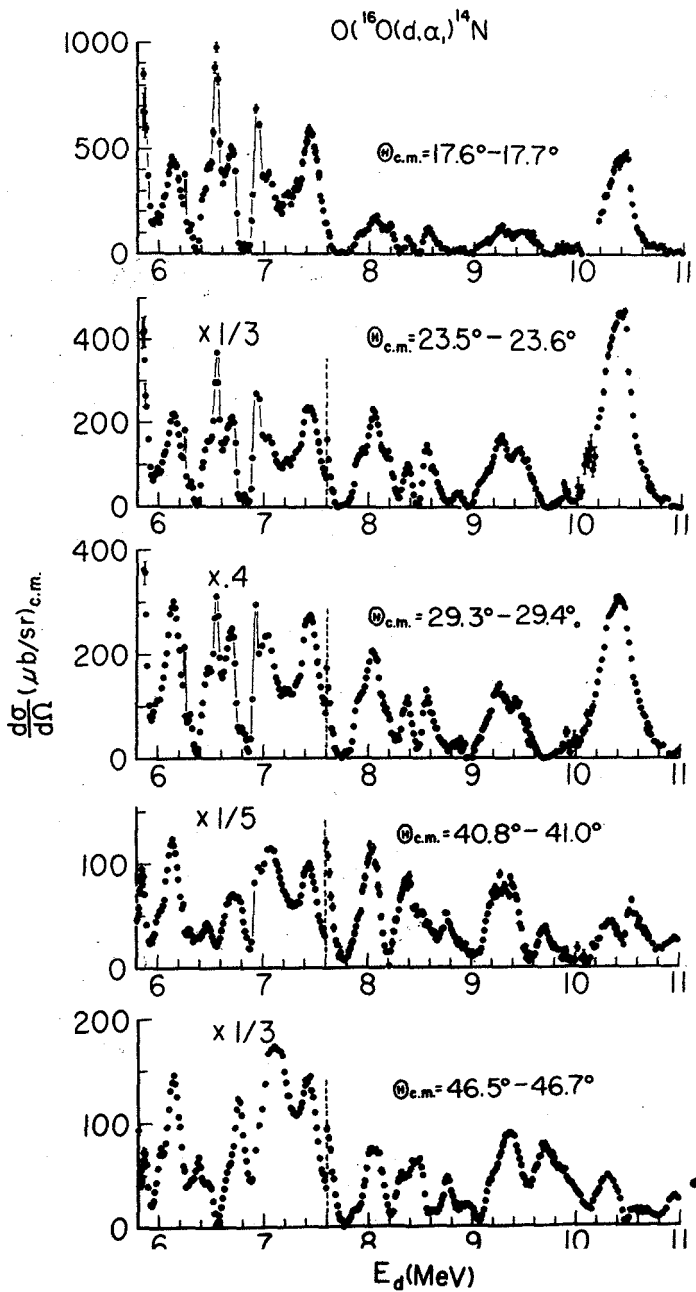


Fig. 7 - Medium energy excitation functions at forward angles.

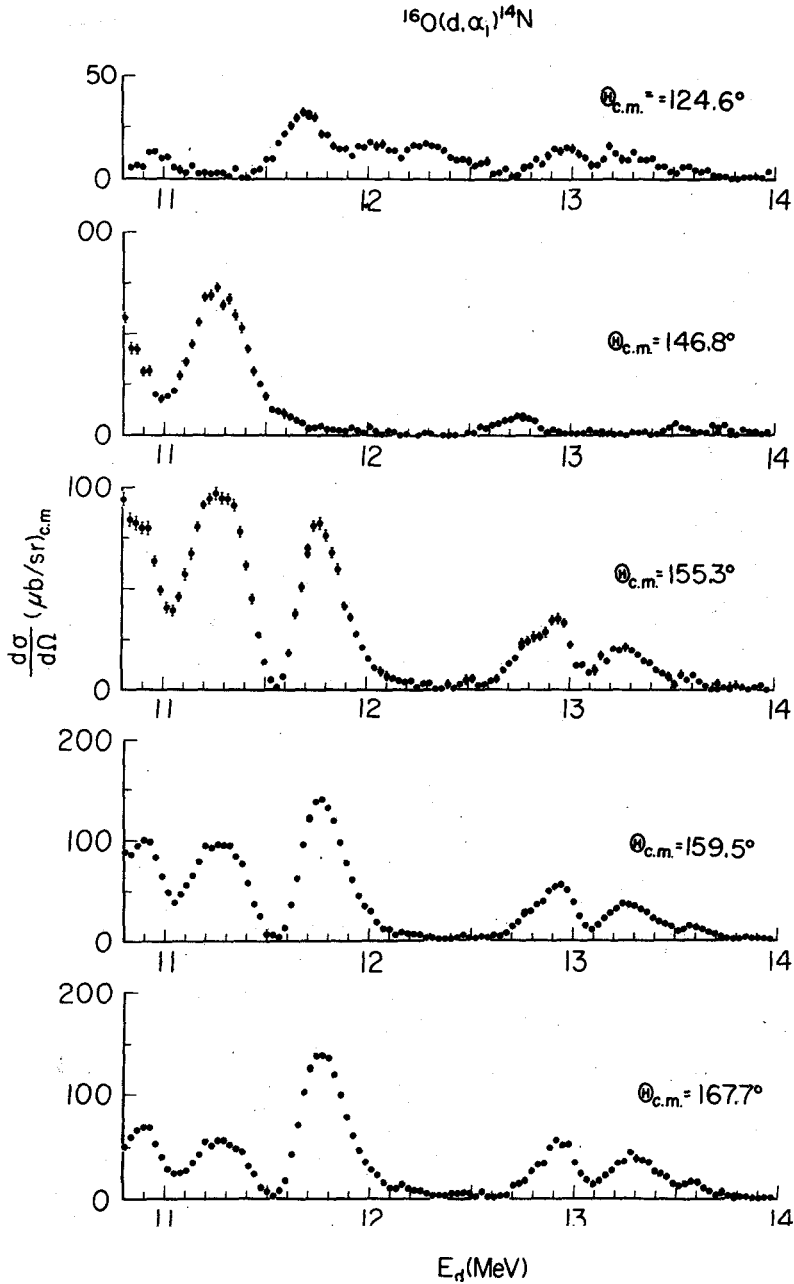


Fig. 8 - Highest energy excitation functions at back angles.

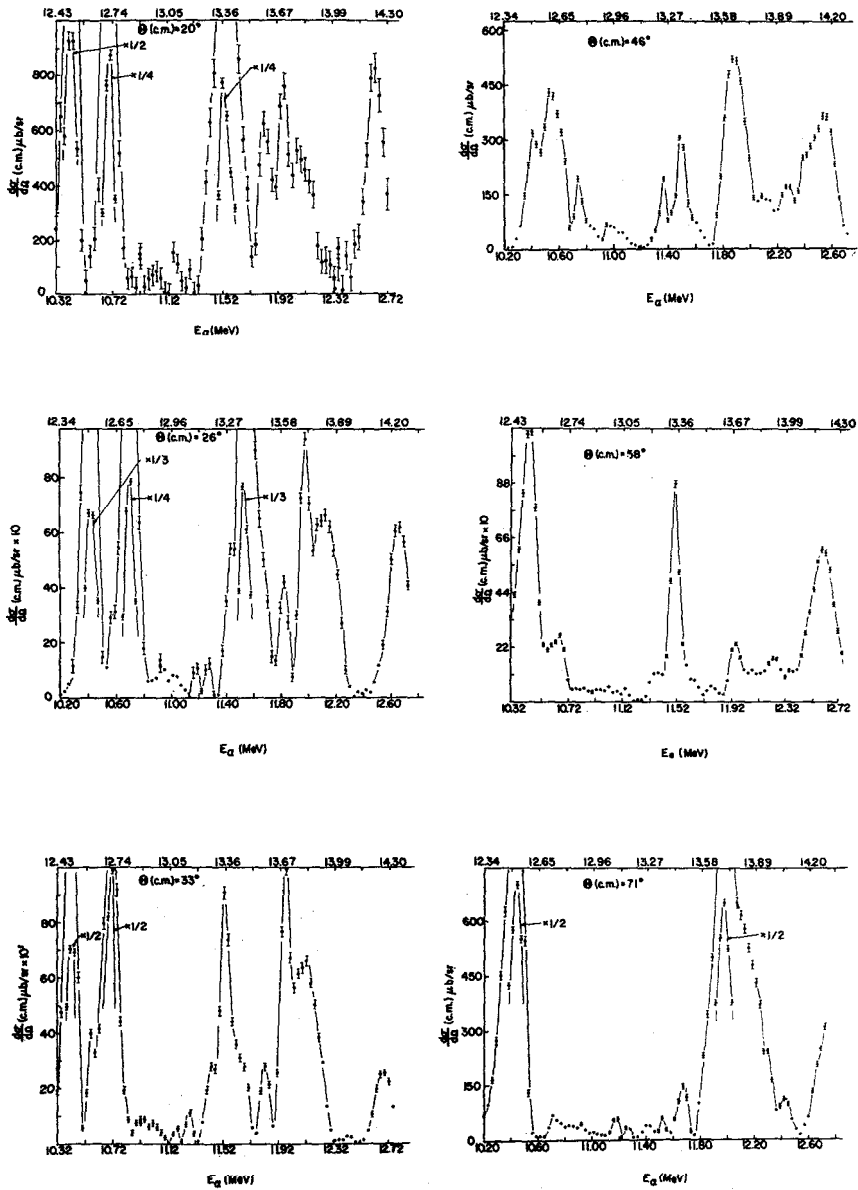


Fig. 9 - Forward angle excitation functions for the $^{14}\text{N}(\alpha, \alpha_1)^{14}\text{N}$ ($T=1$) reaction.

4. Analysis

A. General Remarks

An attractive feature of these reactions is the **simplicity**^{12,13} that results from the fact that **three** of the four particles involved are spin-parity 0^+ and the fourth has **spin** parity 1^+ (This holds for both the $^{16}\text{O} + \text{d}$ **entrance** channel and the $^{14}\text{N} + \text{a}$ channel.) As consequences of this spin-parity combination, angular momentum and parity conservation require that the incident and outgoing orbital angular momentum be the same, that the $l = 0$ wave be rigorously forbidden, and that the only permitted compound nuclear states be **those** with natural parity, i. e., $J^\pi = l^{(-)^l}$ where $l \geq 1$. I remind you that these restrictions have nothing to do with isospin, that they are rigorous, and that they already reduce by **several** fold the expected cross sections.

The differential cross section for such a simple spin-parity system also has an unusually simple **form**¹³:

$$\frac{d\sigma}{d\Omega} = \frac{\lambda^2}{12} \left| \sum_{l=1}^{\infty} (2l+1) [l(l+1)]^{-1/2} S_l dP_l(\cos\theta)/d\theta \right|^2,$$

where l is the orbital angular momentum, $S_l = re^{i\beta_l}$ is the complex S matrix element for the $J^\pi = l^{(-)^l}$ partial wave, and $dP_l(\cos\theta)/d\theta$ is the derivative of the ordinary Legendre **polynomial**. **Let** me also emphasize that this expansion is independent of reaction mechanism. However, where we have resonances and hence compound nucleus formation, the S_l will involve a coherent sum of the resonant contributions from $J = l$ states. If we have a single isolated resonance, (or only one l **contributing**) the angular distribution is simple **and unique**.

In Fig. 10 we plot such angular distributions for different $J = l$ values. These distributions are of course symmetric about 90° . Please note **first** that **all** cross sections vanish at 0° (and of course also at 180°). Also **notice** that **all** even l 's have zero intensity at 90° , while **all** odd l 's have a **maximum** there. Finally, we observe that the number of **maxima** from $0^\circ - 180^\circ$ **just** equals the $l (= J)$ **value** of the resonant state. Hence, for isolated levels the analysis for J^π is trivial. For our case, **isolated** levels rarely occur and even a **very** small amplitude of another partial wave will, by interference, produce large departures from these simple curves. However, some useful qualitative **features** persist, namely the number of lobes remaining usually corresponds well to the **presence** of a dominant partial wave.

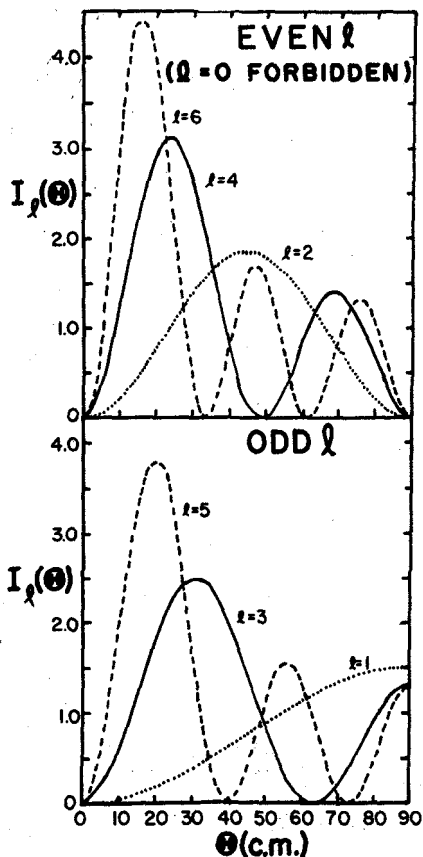


Fig. 10 - Calculated partial wave angular distributions.

B. Application to the $^{16}\text{O}(d, \alpha)^{14}\text{N}$ Data

Figure 11 displays a few of our experimental angular distributions²². One of these ($E_d = 3.820$ MeV) shows very weak interference effects. The two symmetric lobes signal a dominant $l = 2$ resonance (i.e., $J^\pi = 2^+$ for the ^{18}F state) but for the quality of fit shown by the solid curve, we still need a small amplitude of $l = 3$. We will discuss these theoretical curves shortly but first let us note several other interesting distributions on Fig. 11. The three lobed distributions at $E_d = 4.077$ and 7.043 MeV arise from strong $l = 3$ resonances but with a little interference from nearby states of opposite parity to give the asymmetry.

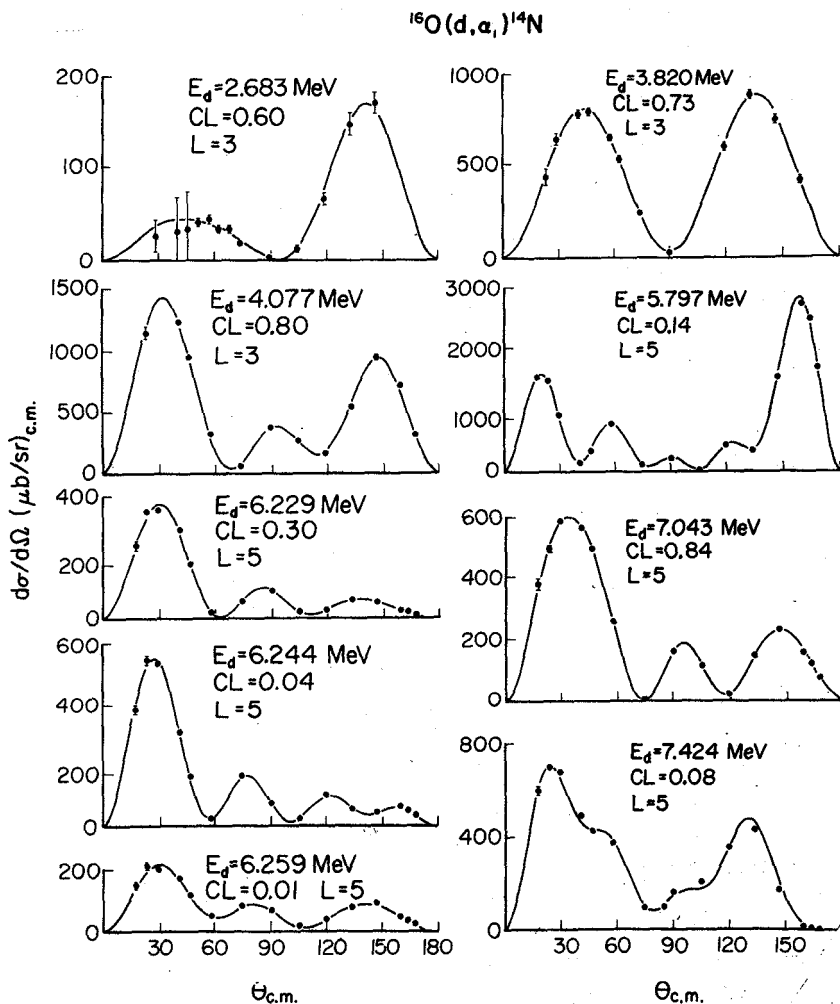


Fig. 11 - A sample of the fitted angular-distributions.

The $E_d = 5.797$ MeV distribution contains the 3000 $\mu\text{barn/sr}$ cross section which I earlier indicated is the largest isospin-forbidden cross section that we have seen via this channel. Most of the intensity here is from a narrow $J = 5^-$ state but tails from nearby 2^+ , 3^- and 4^+ states make significant contributions. However, the characteristic five lobes still remain.

The three distributions at the lower left of Fig. 11 correspond to energies immediately below, **right** on, and immediately above the **single** high point at $E_d = 6.22$ MeV which I called your attention to on the earlier figure showing the **excitation** curves. This **sequence** dramatizes the effect of this narrow (unresolved) 4^+ resonance on the broad strong 3^- level. On either **side** of the one high point the distribution is three lobed but in between, the unresolved resonance **has** enough effect to produce four lobes and by interference **first** to raise the forward cross section from 400 to 600 $\mu\text{b}/\text{sr}$ and then to drop it precipitously to 200 $\mu\text{b}/\text{sr}$ while at 90° (where the even l 's **can** make no contribution) the cross section stays approximately steady at a little less than 100 $\mu\text{b}/\text{sr}$.

To **separate** out quantitatively the interference effects which the last figure shows to be large, we will expand the cross section in partial waves. Such a parametrization with the help of a computer is easy and **efficient** with the partial wave expansion given earlier. In fact, for $E_c < 5.5$ MeV, Jolivet¹¹ seldom **needed** more than three partial waves, i. e., $l_{\text{max}} \leq 3$. At our highest energies ($E_c \sim 14$ MeV), l_{max} sometimes included seven partial waves. The program would converge to a solution rapidly even with random numbers for the starting parameters.

Unfortunately such a parametrization turns out not to be **unique**¹³, except for the l_m wave. This **intrinsic** ambiguity is similar to the well known **Minami** and Fermi-Yang ambiguities for elastic scattering of spin 1/2 by spin zero **particles**. For our case, we have $2^{l_{\text{max}} - 2}$ ambiguous solutions which give different sets of $|S_l|$ s. Not **only** are there ambiguous solutions but at times different sets of solutions may converge and then **separate** or they may cross as a function of energy. In such cases, one can unknowingly **jump** from one solution set to another. While we've not found any completely foolproof way to guarantee staying with one solution set, Jolivet has worked out procedures and tests (described **elsewhere**^{11,14}) which give us considerable **confidence** that we **can** achieve continuous solutions. Even more important, he **has** developed a rationale for choosing the physical solution from an ambiguous **set**¹⁴. A computer experiment **led** him to this selection method. He started by postulating a simple system described by two Breit-Wigner resonances in different partial waves, and then he **generated** all the other ambiguous solutions. These non-physical solutions **turned** out to require many more resonant states of the system than the two **originally** postulated in the physical solution. So we conclude that the correct physical solution is always the simplest. This criterion of course **really** originated with **William of Occam** in the Middle Ages and is known as Occam's razor for **choosing** between hypotheses.

Since Jolivette describes this computer experiment in a recent Phys. Rev. Letter¹⁴, I will not report the details. Instead, let us use it to select a physical solution for the $^{16}O(d, \alpha_1)^{14}N$ data

Figure 12 displays as individual points the computer extracted $\{S_l\}$ elements at low deuteron energies^{11,14} where the l_{max} needed is mainly ≤ 3 . For such a case there are only $2^{l_{max}-2} = 2$ ambiguous solution sets. For one of these sets we use prime labels, e.g. $\{S'_2\}$. Our task will be to decide whether the primed or unprimed set is the correct physical solution. I remind you that $\{S_{l_{max}}\}$ is unique, so we show only one $\{S_3\}$ and we assume that we can stay with this same solution even after $\{S_4\}$ and $\{S_5\}$ become non zero (see last line of figure). Now, for the unique $\{S_3\}$ elements, let us focus our attention on the energies where there are relatively sharp resonances (as shown by the arrows). At energies near these resonances, consider the behavior of set $\{S_1\}$ and $\{S_2\}$ compared to the ambiguous set $\{S'_1\}$ and $\{S'_2\}$. Both of the primed sets qualitatively show more structure than the unprimed set. Hence, by Occam's razor the unprimed set should be the physically correct set. Although these considerations are somewhat qualitative and subjective, when one fits the separate sets of $\{S_l\}$ with resonant states one can demonstrate that many fewer states are needed for the unprimed solution set.

The line through the S matrix elements of the unprimed solution is indeed such a theoretical fit based upon a coherent sum of Breit-Wigner resonances and with no background assumed. Thus

$$|S_l| = \sum_{\lambda} \frac{a_{\lambda} + ib_{\lambda}}{E - E_{\lambda} + i\Gamma_{\lambda}/2}$$

where E_{λ} and Γ_{λ} are the resonant energy and width respectively and $a_{\lambda} + ib_{\lambda} = (\Gamma_d \Gamma_{\alpha})_{\lambda}^{1/2}$, the partial widths for the incoming and outgoing channels. In such a coherent sum, interference effects from other levels of the same spin-parity are very important.

We thus complete our parametrization of the data in terms of a set of level parameters. Fig. 13 summarizes the location, strength $\{S_l\}_{max}$ and the width of the necessary states. Numerical values of the parameters are available in Jolivette's thesis¹⁴ and will be listed in Ajzenberg's forthcoming energy level summary⁷ for $A = 18$.

In discussing any systematics in the levels, let us start with the high spin states first, since the $(2I + 1)$ weighting factor for the cross sections and the

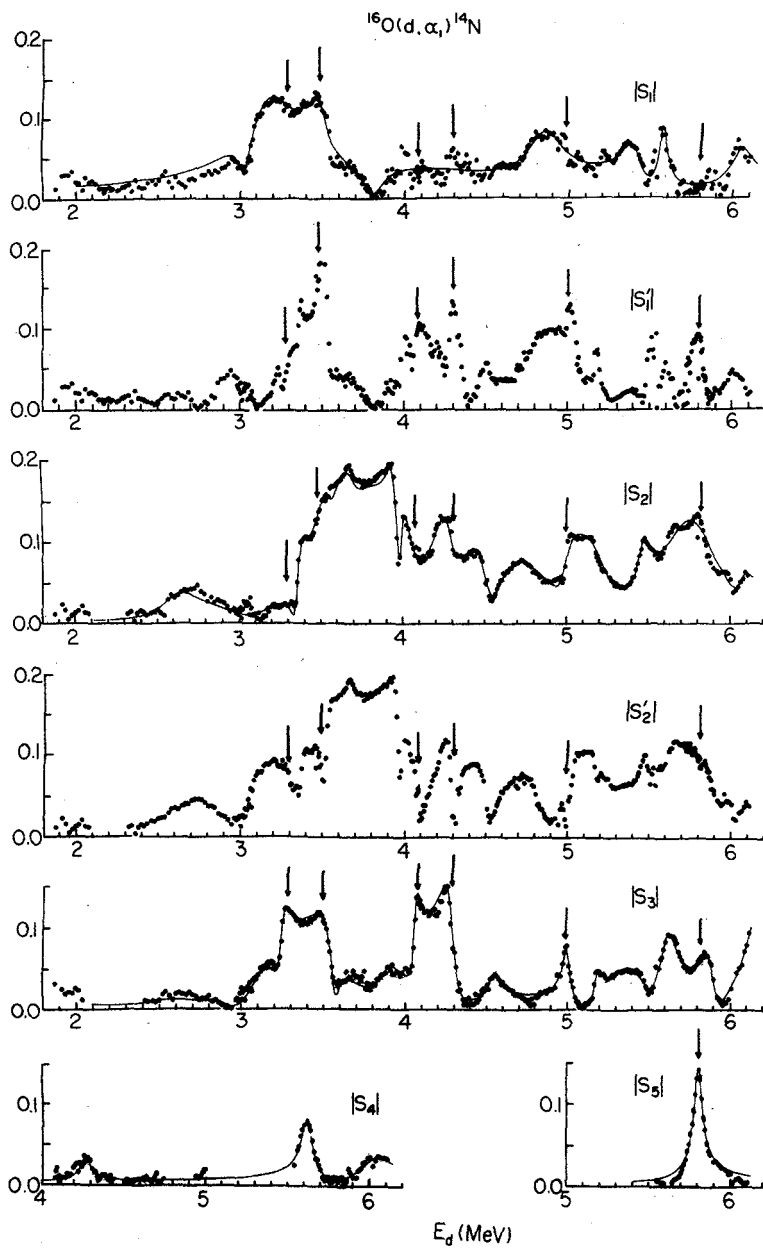


Fig. 12 - Calculated values of the $|S_i|$ elements at low deuteron energies.

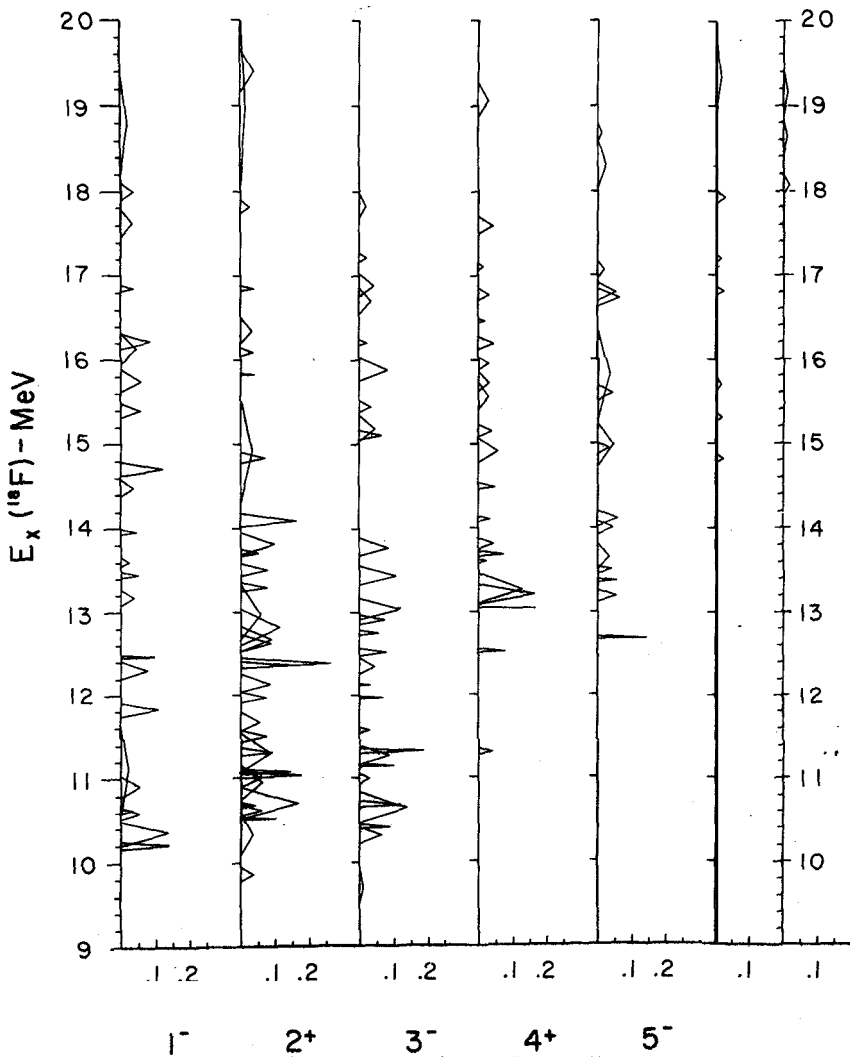


Fig. 13 - Location, strength $|S_l|_{\text{max}}$ and width of states necessary to fit the experimental results.

lack of ambiguity in the highest partial wave means these are the most accurate. The 6^+ and 7^- states first appear at $E, \sim 15$ and 18 MeV, which is not surprising since the penetrability of the centripetal barrier by the outgoing alphas becomes small at much lower excitation energies.

But the density of such high spin states may also be small at lower excitation energies. The first 5^- level $E_x(^{18}\text{F}) = 12.7$ MeV is sharp probably because on the penetrability considerations, since the outgoing $l = 5$ alphas have only 6 MeV in the c.m. system and, as we will see later, the outgoing width dominates the total width for this case. Note that while this level stands alone (isolated by many half widths), all the other 5^- states have close enough neighbors that overlap and interference will be very important.

The lower spin states, 4^+ , 3^- , 2^+ , are similar in showing a region of maximum strength and density of levels. Both strength and density drop off at high and at low excitation energies. This behavior at low energies is consonant with penetrability and level density arguments. At the higher energies the naive explanation might be that isospin conservation starts to reassert itself. However, there are objections to this conclusion which I will discuss later. The 1^- states (whose existence and parameters are least certain) show less variation with energy. If this strength at high energy be a real effect, the probable explanation is that we are well into the giant dipole resonance, so $J^\mu = 1^-$, $T = 1$ states may be substantially enhanced.

C. Application to the $^{14}\text{N}(\alpha, \alpha_1)^{14}\text{N}(T = 1)$ Data

So far we have discussed mainly Jolivette's analysis of ^{18}F seen in his forbidden $^{16}\text{O}(d, \alpha_1)^{14}\text{N}$ data. As I indicated earlier, we may populate the same region of excitation in ^{18}F by using the $^{14}\text{N} + \alpha$ channel. The analogous isospin-forbidden reaction is inelastic alpha scattering leaving ^{14}N in its first excited state which is $T = 1$. Since the spin-parity combinations are exactly the same, all our analysis techniques apply equally well to $^{14}\text{N}(\alpha, \alpha_1)^{14}\text{N}(T = 1)$. Unfortunately our analysis of the inelastic alpha scattering occurred before we were as clever in developing good procedures for staying with the same solution set and in picking a physical solution from the ambiguous sets. Of course, our analysis is unique for the l_{\max} wave. Furthermore, a strong resonance in a lower partial wave will often appear in all solution sets, so our earlier analysis still reveals much useful information about the ^{18}F states involved.

Figure 14 shows a three-dimensional plot of fitted angular distributions¹⁵ over incident alpha energy range from about 10-13 MeV. The corresponding $E_x(^{18}\text{F})$ is about 12-15 MeV. There is of course no ambiguity in the fits since all solutions predict identical cross sections. The vertical scale is such that the maximum cross section is 3500 $\mu\text{b}/\text{sr}$ which is somewhat larger than we saw via the $^{16}\text{O} + d$ channel. Note that four and five lobed

distributions dominate this region though there is a strong enough $J^\pi = 6^+$ level at $E, \approx 11.9$ MeV that the distribution becomes six lobed there.

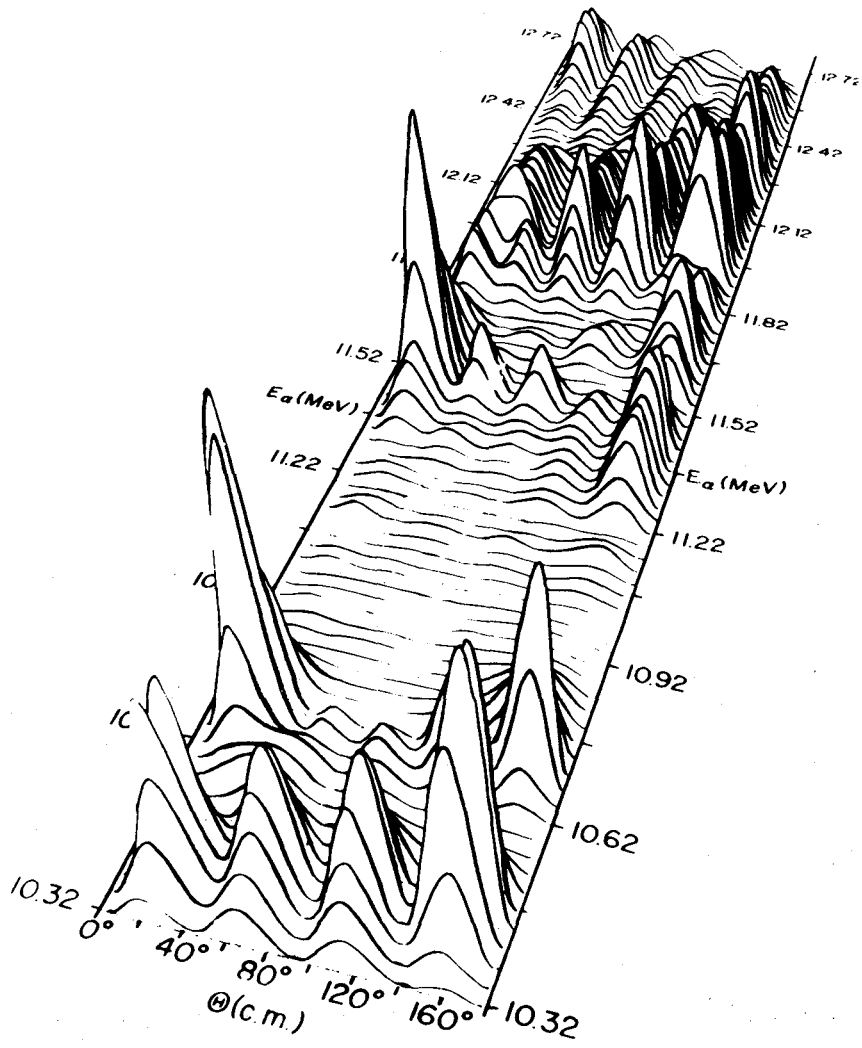


Fig. 14 - Three dimensional plot of angular distributions for the $^{14}\text{N}(\alpha, \alpha_1)^{14}\text{N}$ ($T = 1$) reactions.

The solution set which Tollefsrud selected^{10,15} gives the partial wave cross sections shown in Fig. 15. The number and general character of the high l resonances is the same in all solutions, but we cannot defend all the structure in the $l = 1$ or $l = 2$ waves since we may be on a wrong solution set. Note the doublet structure in the $l = 6$ wave ($J^\pi = 6^+$ states) when it first appears and note for the odd l 's how the $l = 5$ wave ($J^\pi = 5^-$ states) dominate the cross section.

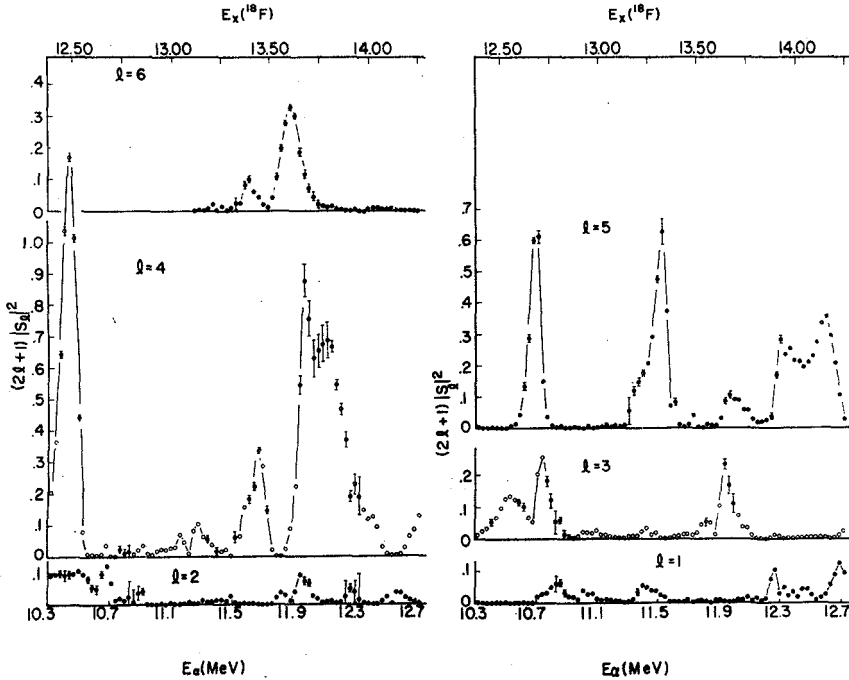


Fig. 15 - Partial wave cross sections for the $^{14}\text{N}(\alpha, \alpha')^{14}\text{N}$ ($T = 1$) reaction calculated by Tollefsrud.

An interesting question occurs as to whether we see the same isospin mixed states in ^{18}F when we enter by the two different channels. Fig. 16 indicates that we certainly do part of the time at least, but of course the relative strengths may be quite different. For example, compare the $l = 4$ resonance in the two channels, but note also the approximate equal strength of the 5^- state seen by either channel. I'll comment on this later.

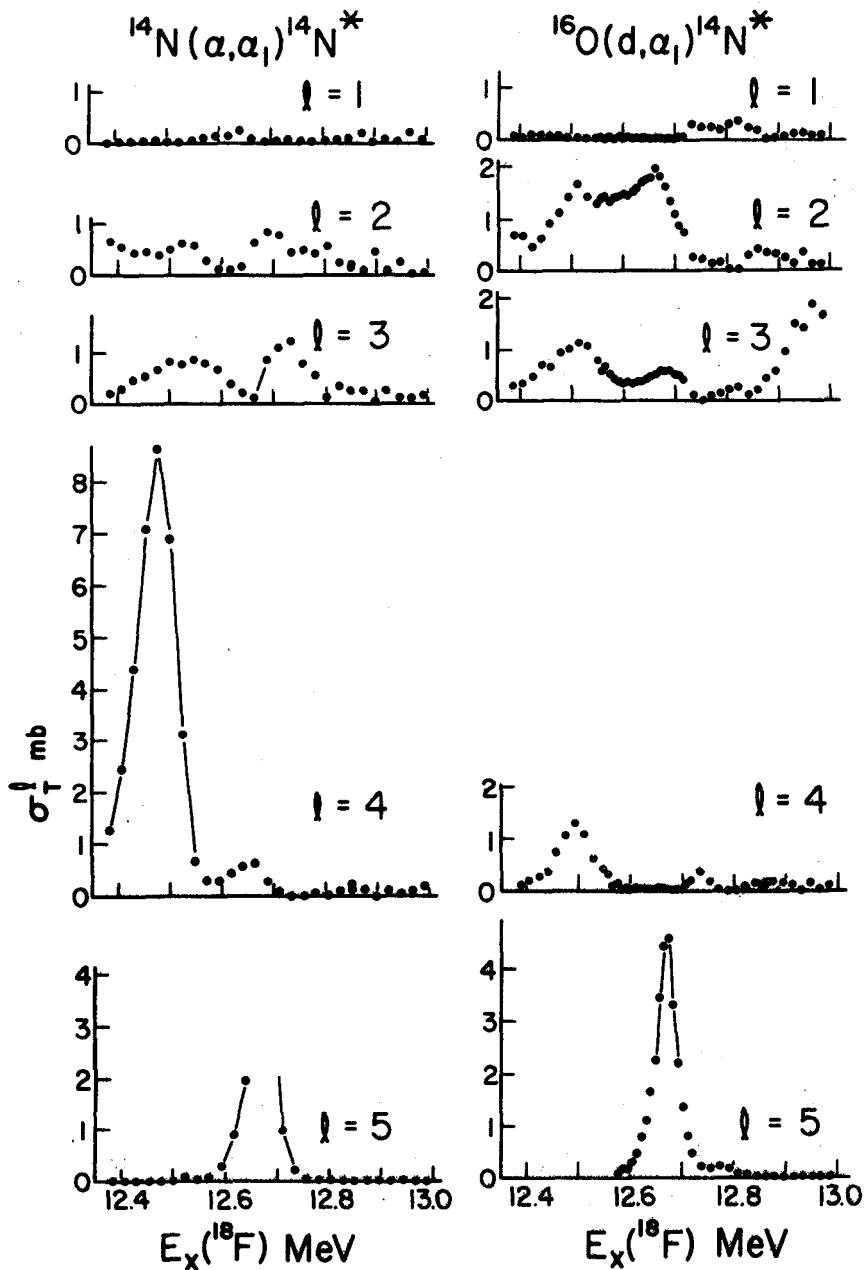


Fig. 16 - Comparison of the partial wave cross sections calculated for the $^{14}\text{N}(\alpha, \alpha_1)^{14}\text{N}^*$ and $^{16}\text{O}(d, \alpha_1)^{14}\text{N}^*$ reactions.

5. Discussion of Results

Thus far we have ignored the question as to why isospin is not conserved in these reactions. The explanation could of course be that nuclear forces are indeed not charge independent, but before thus concluding we should explore whether the known Coulomb force (which is certainly charge dependent) can account for our observations. Theorists calculate that the Coulomb matrix elements H_C are at most only ≈ 100 keV so that the ground and low lying states of the light nuclei should be nearly pure isospin states. The first excited state of the same spin and parity, but different isospin, always lies many millions of electron volts away, so the impurity estimates produced by the Coulomb matrix elements are generally predicted to be $\ll 1\%$. Furthermore, we have seen, in our case at least, that the forbidden cross section show no appreciable direct interaction; in fact all the the data parametrizes in terms of compound nuclear resonances without even the need of any background contribution. Therefore we must look to the compound state as the primary source of isospin violation. At these excitation energies and level densities, there is no longer always a large energy gap between states of the same spin-parity but different isospin. In fact, for our odd-odd self conjugate nucleus ^{18}F , the $T = 1$ states start within an MeV of the $T = 0$ ground state. By 10 MeV excitation energy, the density of $T = 0$ and $T = 1$ levels may well be high enough that occasionally some states of the same spin-parity may be close enough and the state may live long enough that the Coulomb matrix element can introduce appreciable isospin impurities into the state. This prediction Wilkinson¹⁶ made soon after Adair's classic paper. However, the wholesale mixing that we see in ^{18}F is surprising if the levels of the same spin-parity but different isospin were really randomly distributed. There is, in fact, some evidence in light self conjugate nuclei that often there may be relatively close doublets of the same spin-parity but of different isospin. These isospin doublets arise because these states have appreciable cluster components which mirror each other. Best publicized are the ^8Be doublets (2^+ , 1^+ , 3^+) where for the 2^+ pair, Marion et al.¹⁷ have shown the states to be primarily the mirror clusters $Li^7 + p$ and $^7\text{Be} + n$ and consequently the isospin-mixing is near maximum. The mirror cluster components explain why energetically the states lie close together and have large isospin impurity.

We suspect that in ^{18}F this is a rather common phenomenon. In fact, Marion¹⁸ has reported in ^{18}F such a pair even at very low excitation energy: the 1^- isospin doublet at 5.59 and 5.66 MeV.

If in ^{18}F such doublets with appreciable mirror cluster configurations are common, we should often see both members in our forbidden reactions. We could label these as mirror or intrinsic doublets, in contrast to those from unrelated configurations which accidentally lie close enough that the Coulomb forces can mix the isospins. In the latter case, we would not necessarily expect the yields from the doublet members to be comparable. In fact, one state may well have too small a partial width to observe. The result would be a single isolated resonance. We probably have examples of both though as the level density increases the mirror configurations may be spread over many levels, so doublets become multiplets. For example, consider the 5^- states in Fig. 13. The strong 5^- resonance at $E_r = 12.7 \text{ MeV}$, which we have mentioned several times, stands isolated many half widths away from any other 5^- level. All our other 5^- resonances however lie within a half-width of one or more similar levels. We cannot exclude the possibility that the apparently isolated 5^- level is in fact a very close doublet. The $|S_5|$ curve for this resonance is slightly asymmetric. A close doublet would help account for the high yield.

Wilkinson¹⁶ also predicted that, as the excitation energy increased, isospin conservation should reestablish itself because as more channels open, the total width increases until the lifetime finally becomes shorter than the characteristic Coulomb mixing time $\frac{\hbar}{H_c}$. So, if the system starts with a well defined isospin, the final system must have the same isospin. He expected the threshold for this region to be between 14 and 18 MeV excitation in ^{18}F . Our data already extends to 20 MeV excitation and we still see resonances although it is true that the cross sections are much reduced. However, the allowed cross sections are also decreasing, so the relevant quantity is the ratio of forbidden to allowed cross sections as a function of energy. When these are plotted, there is no indication that isospin conservation reasserts itself. Carol Chesterfield and P. D. Parker¹⁹ at Yale have recently extended our forbidden $^{14}\text{N}(\alpha, \alpha_1)^{14}\text{N}$ data to the higher energies available on the Yale MP Tandem and even at 25 MeV excitation energy in ^{18}F they see strong resonances for the isospin-forbidden alphas. Apparently, there are still large numbers of long lived ^{18}F states even at these excitation energies.

In general, for our isospin mixed states we cannot distinguish between a predominantly $T = 0$ state with small $T = 1$ admixture and a predominantly $T = 1$ state with some $T = 0$ admixture. There are exceptions. The strong 5^- state at $E_r = 12.7 \text{ MeV}$ comes at precisely the right energy to be the analog of a 5^- state in ^{18}O which has been identified at the TUNL²⁰

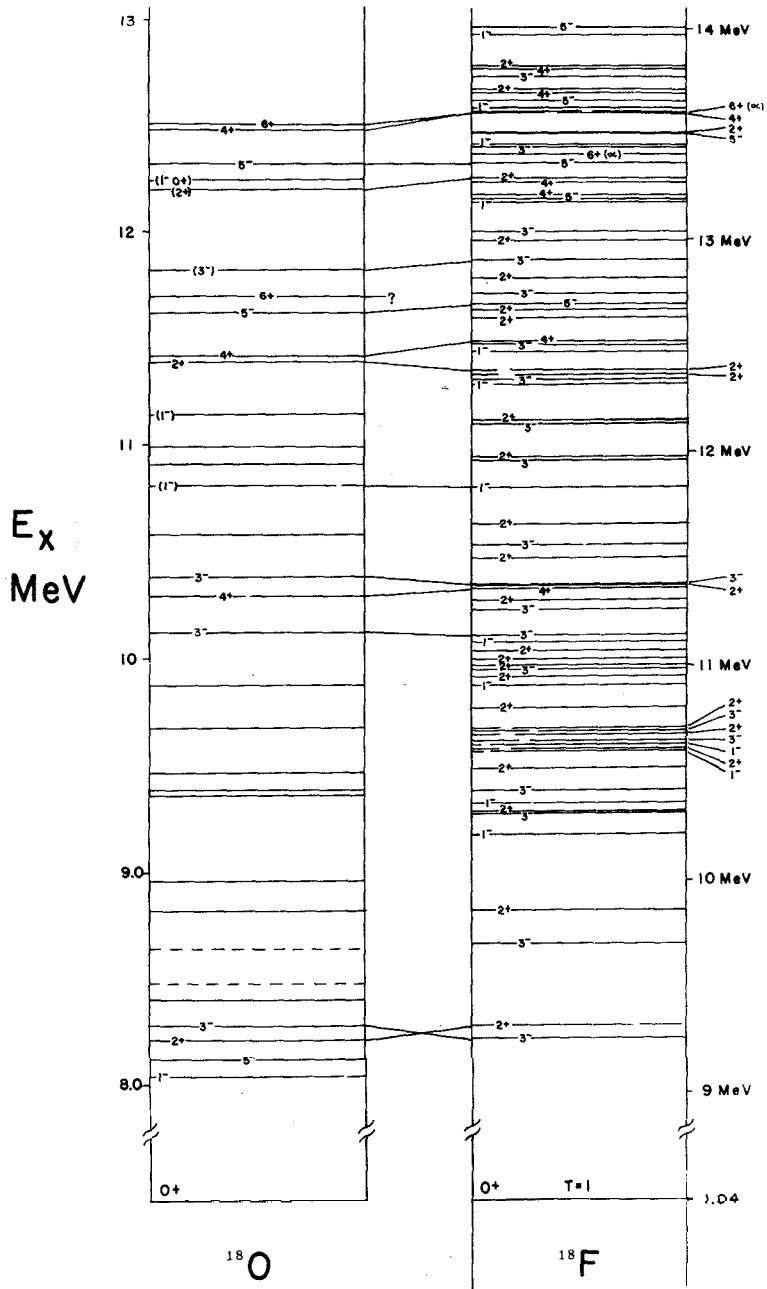


Fig. 17 - States of the mass 18 isobars showing some of the analogues.

Laboratories by **elastic** scattering of **alphas** by ^{14}C . Fig. 17 shows such ^{18}O levels and some of the analogues in ^{18}F from our work. With few exceptions, wherever they see a strong level in ^{18}O via $^{14}\text{C} +$ a scattering, we find the analog state in ^{18}F . **One** exception is the analog to the low energy 6^+ state of ^{18}O (marked with "?"). This **absence** is consistent with the small penetrability associated with the low energy outgoing $l = 6$ alpha particle. We suspect that these analog states are **primarily** $T = 1$ states with some $T = 0$ mixing. Many of the other states probably are $T = 0$ with some $T = 1$ admixture. Of course, level shifts could lead us astray and some ^{18}O states may **remain** undiscovered.

However, in the case of the 5^- level at $E_r = 12.7$ MeV, we have further confirmation of our $T = 1$ assignment. By luck the angular distribution of the **allowed** reactions, (d, α) , requires **no** coefficient for $P_{1,0}(\cos \theta)$ although such is necessary at higher and lower energies. Hence, we **infer** that no $T = 0$, $J^\pi = 5^-$ state contributes **significantly** at this energy to the allowed (d, α_0) cross section. Therefore $\Gamma_{\alpha_0} < \Gamma$ for this resonance.

But $|S|^2_{max} = 4 \frac{\Gamma_{in}\Gamma_{out}}{\Gamma^2}$, so to **obtain** the nearly equal $|S_5|$ for both the deuteron and alpha channel requires $\Gamma_d \approx \Gamma_{\alpha_0}$. Hence, both must be $\ll \Gamma$. The only other allowed channels that have appreciable yield do not show this resonance. Hence we assume $\Gamma \approx \Gamma_d + \Gamma_{\alpha_0} + \Gamma_{\alpha_1} \approx \Gamma_{\alpha_1}$, where Γ_{α_1} is the partial width to the forbidden $T = 1$ state. Thus the forbidden exit channel accounts for most of the total width. If the ^{18}F state were predominantly $T = 1$, we should expect this since at this energy the α_1 channel would be the only effective mode of decay.

References

1. W. Heisenberg, *Z. Phys.* **77**, 1, (1932).
2. G. Breit and E. Feenberg, *Phys. Rev.* **50**, 850 (1963).
3. E. Wigner, *Phys. Rev.* **51**, 106 (1937).
4. R. Adair, *Phys. Rev.* **87**, 1041 (1952).
5. F. Ajzenberg-Selove, *Nucl. Phys.* **A152**, 1 (1970).
6. C. P. Browne, *Phys. Rev.* **104**, 1661 (1956).
7. F. Ajzenberg-Selove, *Nucl. Phys.* (in press).
8. R. G. Herb, U. S. Patent 2-816-243-ChargeExchange Method of **Negative Ion Production** (1957).
9. K. G. McKay, *Phys. Rev.* **76**, 1537 (1949), first successfully used **reverse** biased diodes for detection of charged particles, but another decade passed before the technology developed to the state where these detectors were suitable for many nuclear physics applications.
10. P. Tollefsrud, Ph. D. Thesis. Univ. of Wisconsin (Available through University Microfilms. Ann Arbor, Michigan (1969).

11. P. Jolivette, Ph. D. Thesis, Univ. of Wisconsin (Available through University Microfilms, Ann Arbor, Michigan (1970).
12. J. Jobst, S. Messelt and H. T. Richards, Phys. Rev. 178, 1663 (1969).
13. P. Jolivette and H. T. Richards, Phys. Rev. 188, 1660 (1969).
14. P. Jolivette, Phys. Rev. Letters 26, 1383 (1971).
15. P. Tollefsrud and P. Jolivette, Phys. Rev. C1, 398 (1970).
16. D. H. Wilkinson, Phil. Mag, 1, 379 (1956).
17. J. B. Manon, Nucl. Phys. 68, 463 (1965); J. B. Marion and M. Wilson, Nucl. Phys. 77, 129 (1966).
18. J. B. Marion, in *Nuclear Research with Low Energy Accelerators*, ed. by Marion and Van Patten, Academic Press. New York (1967), p. 501.
19. C. M. Chesterfield and P. D. Parker, Bull. Am Phys. Soc. 15, 1654 (1970).
20. G. L. Morgan, D. R. Tilley, G. E. Mitchell, R. A. Hilki and N. R. Roberson, Nucl. Phys. A148, 480 (1970).